

## *Retraction*

# **Retracted: Research on Spectrum Feature Identification of Indoor Multimodal Communication Signal**

### **Advances in Mathematical Physics**

Received 19 December 2023; Accepted 19 December 2023; Published 20 December 2023

Copyright © 2023 Advances in Mathematical Physics. This is an open access article distributed under the Creative Commons Attribution License, which permits unrestricted use, distribution, and reproduction in any medium, provided the original work is properly cited.

This article has been retracted by Hindawi following an investigation undertaken by the publisher [1]. This investigation has uncovered evidence of one or more of the following indicators of systematic manipulation of the publication process:

- (1) Discrepancies in scope
- (2) Discrepancies in the description of the research reported
- (3) Discrepancies between the availability of data and the research described
- (4) Inappropriate citations
- (5) Incoherent, meaningless and/or irrelevant content included in the article
- (6) Manipulated or compromised peer review

The presence of these indicators undermines our confidence in the integrity of the article's content and we cannot, therefore, vouch for its reliability. Please note that this notice is intended solely to alert readers that the content of this article is unreliable. We have not investigated whether authors were aware of or involved in the systematic manipulation of the publication process.

Wiley and Hindawi regrets that the usual quality checks did not identify these issues before publication and have since put additional measures in place to safeguard research integrity.

We wish to credit our own Research Integrity and Research Publishing teams and anonymous and named external researchers and research integrity experts for contributing to this investigation.

The corresponding author, as the representative of all authors, has been given the opportunity to register their agreement or disagreement to this retraction. We have kept a record of any response received.

### **References**

- [1] Y. Chen, Y. Liu, and X. Fan, "Research on Spectrum Feature Identification of Indoor Multimodal Communication Signal," *Advances in Mathematical Physics*, vol. 2021, Article ID 7913666, 9 pages, 2021.

## Research Article

# Research on Spectrum Feature Identification of Indoor Multimodal Communication Signal

Yunfei Chen <sup>1,2</sup>, Yang Liu <sup>1,2</sup> and Xintao Fan<sup>1,2</sup>

<sup>1</sup>School of Electrical Engineering, Hebei Vocational University of Technology and Engineering, Xingtai 054035, China

<sup>2</sup>School of Electrical Engineering, Xingtai Polytechnic College, Xingtai 054035, China

Correspondence should be addressed to Yang Liu; [yl20210519@163.com](mailto:yl20210519@163.com)

Received 22 May 2021; Revised 19 August 2021; Accepted 2 November 2021; Published 16 November 2021

Academic Editor: Naixue Xiong

Copyright © 2021 Yunfei Chen et al. This is an open access article distributed under the Creative Commons Attribution License, which permits unrestricted use, distribution, and reproduction in any medium, provided the original work is properly cited.

In order to solve the problem of large signal acquisition error caused by radio wave multipath effect in indoor environment, firstly, the signal source carried on the motion platform is collected for spectrum signal, and the signal processed by wavelet threshold denoising algorithms extracted and stored for spectrum feature extraction. Then, after data training and identification, the signal source is input into the system in random mode for identification. The experimental results show that the improved fuzzy clustering algorithm (FCA) is 12.7% higher than the spectrum envelope extraction method (SEEM) in the recognition rate of spectrum characteristics of different modes of signal source.

## 1. Introduction

In indoor positioning of motion platform, communication signal mode plays a key role in information exchange. Due to the characteristic of indoor radio wave transmission [1] of different modes of communication signal, the working mode can be automatically changed to adjust the channel when the communication [2] is not smooth. The positioning access point AP can identify the signal source on the sports platform to strengthen the positioning and tracking. The spectrum feature identification method is very important for the identification of wave signal is very important. The traditional envelope spectrum feature extraction method [3] can optimize the selection of signal source spectrum features [4] and effectively improve the signal detection accuracy of signal source. However, the feature extraction of the SEEM algorithm is easily limited by the experimental environment. When the indoor environment changes greatly, the error of feature data extracted by the SEEM algorithm is large.

The FCA is a clustering algorithm based on the fuzzy system theory [5]. Bezdek proposed the FCA [6] as early as 1973, which originated from the improved early K-means clustering algorithm. The objective function constructed by the FCA can achieve the maximum similarity of samples

belonging to the same cluster and the minimum correlation of samples between different clusters in the division process. However, the randomness of the FCA clustering center is large, which easily leads to local extremum [7]. At the same time, when the attributes of test samples are close to each other, it is difficult to classify them. All these need to guide the classification. The improved FCA based on pairwise regression fusion can be combined with the FCA in fuzzy classification, so as to improve the classification efficiency.

## 2. Related Work

The method of analyzing the signal characteristics by using the spectrum of the space wave signal received by the spectrum analyzer receiver has been successfully applied in many fields. At present, some scholars have studied the spectrum characteristics of outdoor GPS satellite signal [8], radar signal, and radio signal. However, there are few studies on the spectrum characteristics of indoor interference signal source. In Reference [9], the distortion of the emitter modulator and the nonlinear characteristics of the power amplifier are introduced into the classifier construction model, and the test results show that the spectrum distortion of the emitter signal exists. In Reference [10], the transient sparse feature

of signal is used as the basis of evaluation mode to realize the identification of emitter signal feature. In Reference [11], the relevant features are extracted by analyzing the time-frequency characteristics of the emitter signal to realize the identification of transient characteristics. The above research results are significant, but none of them is involved in the research of indoor positioning signal source spectrum characteristics.

### 3. Methodology

**3.1. Building Models.** In order to solve the problem of large signal acquisition error caused by the multipath effect of indoor signal source, firstly, the spectrum of the radio signal is collected and processed on the indoor platform, and then, the random signal is input to the system to identify the large-scale signal. At last, the construction of signal acquisition and identification system is shown in Figure 1.

The known communication signal source is collected and input into the spectrum identification system by the SA44B spectrum analyzer. According to the four common communication modes of GSM, CDMA, DCS, and PHS, the corresponding spectrum features are extracted and stored in the database after signal detection feature extraction and identification. Then, after learning and training, a higher frequency spectrum feature recognition rate is achieved. In the online identification stage, the signal source with unknown working mode is input into the identification system, and the working mode of the output signal source is determined after identification.

**3.2. Signal Acquisition and Processing.** This section is to distinguish the source signal of the target for positioning; the four modes of spectrum signals of the signal source carried by the indoor sports platform are collected indoors. The spectrum of CDMA signal source has the characteristics of smooth waveform and obvious peak, as shown in Figure 2. The spectrum of signal source in GSM mode is coarser than that in CDMA mode, but it has clear peak, as shown in Figure 3. The spectrum of DCS working mode is the most disordered among the four kinds of spectrum collected, as shown in Figure 4. In PHS mode, the peak to peak distance of communication signal spectrum is larger, so the characteristics are more obvious, as shown in Figure 5.

Obviously, the characteristics of the four modes of spectrum signals are complex, the optimal characteristic parameters of the spectrum are not easy to select, and there are many clutters in the spectrum, which affect the indoor positioning of the signal source.

In order to prevent the edge information from blurring, a nonlinear filter is introduced, in which the median filter can keep the sharp edge well. The signal processed by median filter still contains noise, and the wavelet denoising method is better for reducing Gaussian white noise in radio wave signal. The wavelet denoising method [12] includes the modulus extremum denoising method, wavelet correlation denoising method, and wavelet threshold denoising method. The traditional wavelet hard thresholding function [13] and

soft thresholding method [14] models are shown in

$$\widehat{W}_{j,k} = \begin{cases} \operatorname{sgn}(W_{j,k}) \cdot (|W_{j,k}| - \lambda), & |W_{j,k}| \geq \lambda, \\ 0, & |W_{j,k}| < \lambda, \end{cases} \quad (1)$$

$$\widehat{W}_{j,k} = \begin{cases} W_{j,k}, & |W_{j,k}| \geq \lambda, \\ 0, & |W_{j,k}| < \lambda. \end{cases}$$

The traditional wavelet hard thresholding function is easy to produce Gibbs oscillation [15], while the soft thresholding method is easy to produce “over smooth” distortion due to the constant difference of wavelet coefficients [16].

$$\widehat{W}_{j,k} = \begin{cases} aW_{j,k} + (1-a) \operatorname{sgn}(W_{j,k}) \cdot \left( |W_{j,k}| - \frac{\lambda}{\exp(|W_{j,k}| - \lambda)^\delta} \right), & |W_{j,k}| \geq \lambda, \\ 0, & |W_{j,k}| < \lambda. \end{cases} \quad (2)$$

As shown in formula (2), the threshold adjustment parameter  $a$  is  $a = 1 - e^{-\alpha(|W_{j,k}| - \lambda)^2}$ ,  $W'$  is the mean value of neighborhood wavelet coefficients, and  $\delta$  is a positive number. When  $e|W_{j,k}| \rightarrow \pm\lambda$  is  $\widehat{W}_{j,k} \rightarrow 0$ , the threshold value  $W_{j,k} = \pm\lambda$  function is continuous, which can overcome the signal oscillation problem caused by the discontinuity of hard threshold; when  $W_{j,k} \rightarrow \pm\infty$  is  $\widehat{W}_{j,k}/W_{j,k} \rightarrow 1$ , the new threshold function conforms to the characteristics of hard threshold function, which can overcome the hard threshold, so as to overcome the distortion caused by the constant difference of wavelet coefficients.

When the threshold adjustment parameters  $\alpha \rightarrow 0$  and  $\delta \rightarrow 0$ , the new wavelet threshold function is a soft threshold function; when the threshold adjustment parameters  $\alpha \rightarrow +\infty$  and  $\delta \rightarrow 1$ , the new wavelet threshold function is a hard threshold function. By adjusting the parameters  $a$  and  $\delta$ , we can obtain the signal processing results of different modes of the interference signal source. After denoising the spectrum of the four modes, we can normalize the Z-score [17], as shown in Figure 6.

**3.3. Spectrum Feature of Signal Extraction.** The signal spectrum parameters are selected to extract the peak value, corresponding frequency, signal spectrum bandwidth, and kurtosis [18] of the signal transmitted by different mode signal sources as the characteristic parameters of the corresponding mode of the radio wave signal. The feature parameters of different modes of CDMA, GSM, DCS, and PHS of signal source are extracted step by step to construct the vector sequence required for the feature recognition model of radio wave signal. As shown in Table 1, the four modes of CDMA, GSM, DCS, and PHS are, respectively, marked as  $C = 1 \sim 4$ .

**3.4. Analysis of Category Characteristics.** Let the length of eigenvectors in feature set  $X = \{x_1, x_2, \dots, x_n\}$  be  $l$ , and the number of eigenvectors be  $n$ ; then, feature set  $X$  is divided into  $c$  fuzzy groups. In order to represent the degree to which

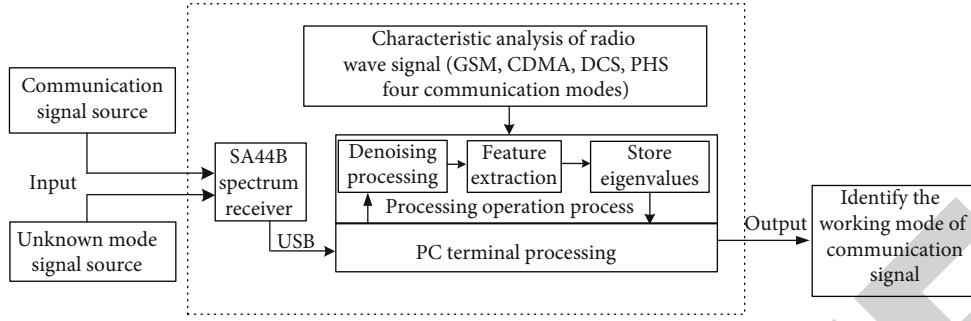


FIGURE 1: Structure diagram of signal acquisition and identification system.

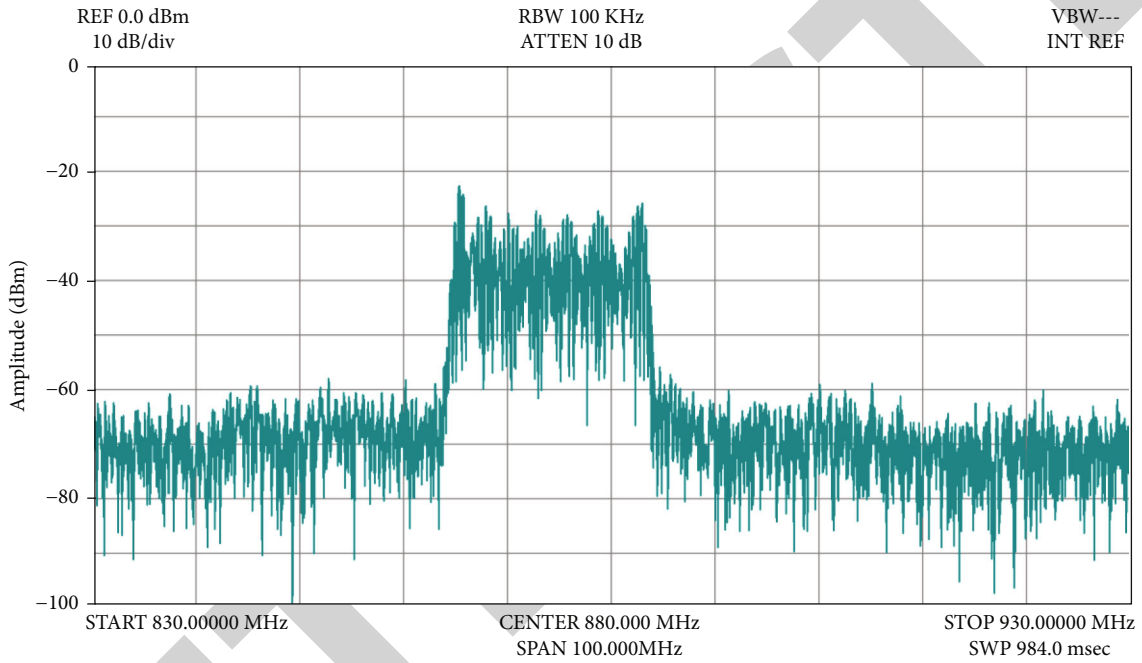


FIGURE 2: Spectrum of CDMA mode.

each eigenvector belongs to  $c$  independent classes, the algorithm returns  $c$  clustering center matrix and membership matrix  $U_{c \times n} = \{u_{ij}\}$ , where each element  $u_{ij}$  indicates that  $x_i$  of  $\mathbf{X}$  belongs to  $c_j$  membership. The objective function is constructed as follows:

$$F_{fcm}(u, c) = \sum_{j=1}^n \sum_{i=1}^c u_{ij}^m d_{ij}^2(x_j, c_i), \quad (3)$$

$$\text{s.t. } \sum_{i=1}^c u_{ij} = 1, \quad \forall j = 1, \dots, n.$$

Taking each row of feature set in Table 1 as the corresponding feature vector, the feature vector matrix of  $M \times N = 4 \times 8$  can be constructed, and  $\mathbf{X}$  is the input matrix of the fuzzy clustering algorithm. The number of clusters is set as  $c = 4$ , the fuzzy weight parameter is  $m = 2$ , the number

of iterations is 500, and the iteration stop threshold parameter is  $\epsilon = 1.0 \times 10^{-5}$  by four modes. The cluster center set  $C$  and membership matrix  $U$  of four kinds of eigenvectors can be obtained by operation.

As shown in formula (3),  $C$  is the cluster center set,  $c_i$  is the cluster center of class  $i$ ,  $m$  is the fuzzy weight parameter,  $D$  is the initial number of clusters in fuzzy clustering,  $m = 2$  according to experience, and  $d_i(x_i, c_i) = \sqrt{\sum_i^n (x_i - c_i)^2}$  is the Euclidean distance from feature vector  $x_i$  to class center  $c_i$ . Through iterative calculation, the data is close to the optimal clustering center  $C = \{c_i\}$ .

$$C = \begin{bmatrix} 3.7853 & 0.4924 & 1.2582 & 1.3613 \\ 6.3072 & 0.5661 & 1.3713 & 1.8426 \\ 3.6519 & 0.6368 & 1.0911 & 1.1998 \\ 4.8730 & 0.6689 & 1.3461 & 1.3791 \end{bmatrix},$$

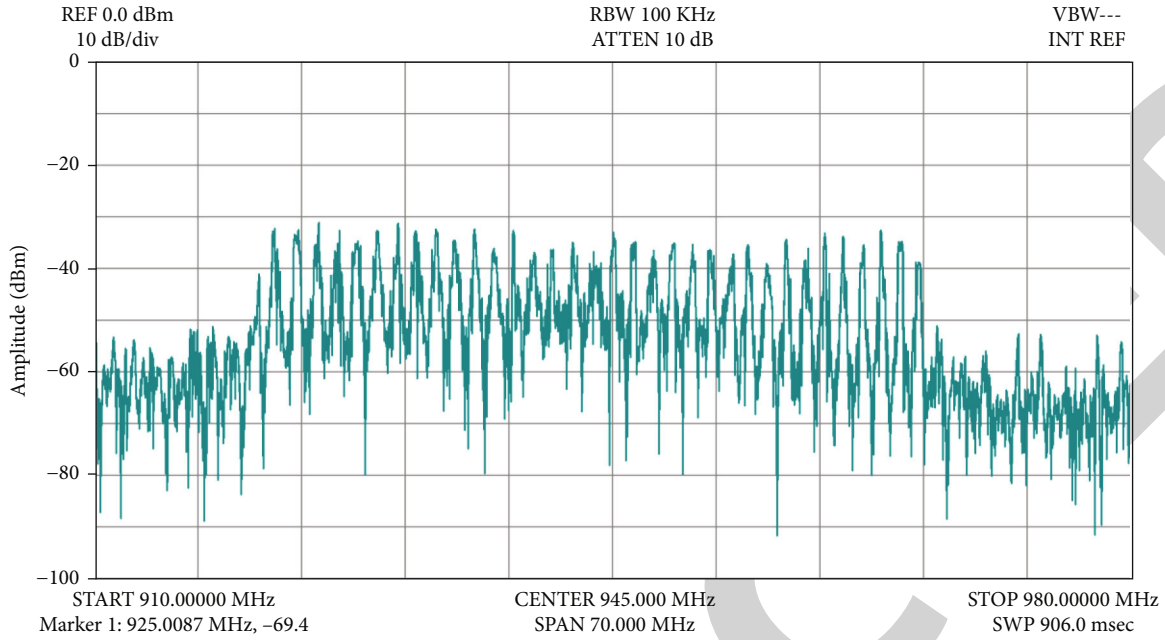


FIGURE 3: Spectrum of GSM mode.

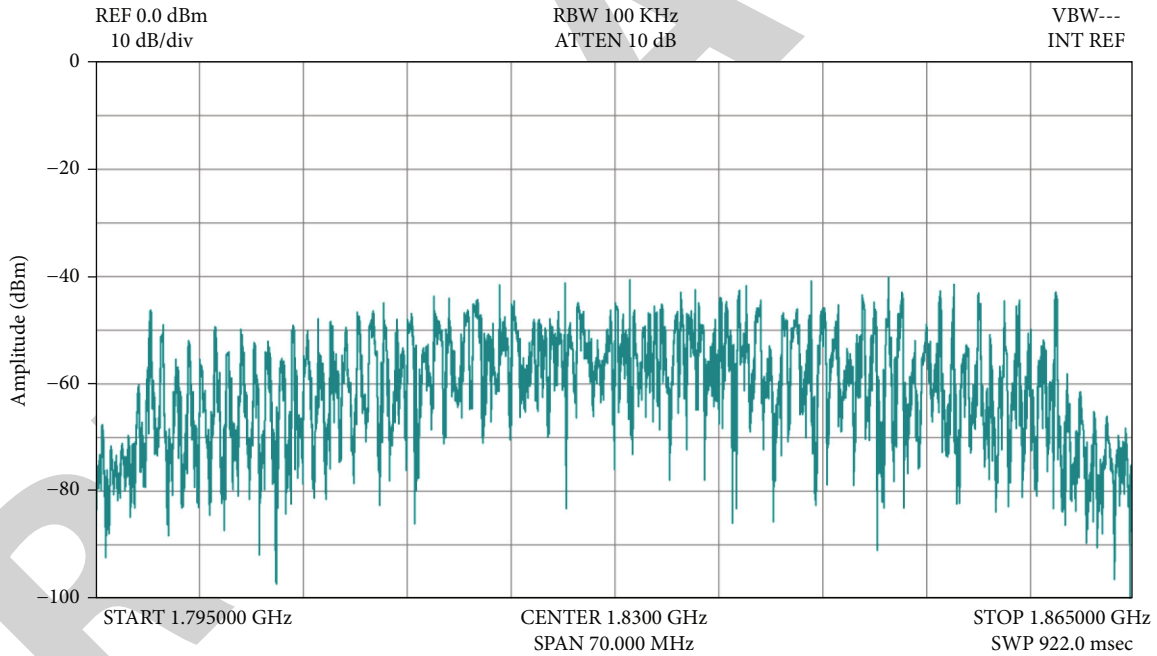


FIGURE 4: Spectrum of DCS mode.

$$U = \begin{bmatrix} 0.9861 & 0.9994 & 0.0065 & 0.0296 & 0.0001 & 0.0127 & 0.0074 & 0.0090 & 0.0000 \\ 0.0018 & 0.0000 & 0.9713 & 0.8936 & 0.0002 & 0.0115 & 0.0097 & 0.0007 & 0.0001 \\ 0.0082 & 0.0002 & 0.0032 & 0.0172 & 0.0000 & 0.0060 & 0.0025 & 0.9802 & 0.9999 \\ 0.0074 & 0.0003 & 0.0268 & 0.0726 & 0.9997 & 0.9707 & 0.9834 & 0.0020 & 0.0000 \end{bmatrix} \quad (4)$$

From the data in the membership matrix  $U$ , we can find the row number to which the eigenvector belongs, that is,

the membership degree of the class label. The row code corresponding to the maximum value in each column of data is the category number to which the eigenvector belongs. According to matrix  $U$ , the maximum data values calculated in columns 1 ~ 2 appear in the first row, so the characteristic data in columns 1 ~ 2 in Table 1 are classified into the same category. Approximately, according to the maximum membership value of the characteristic data in columns 3 ~ 4, 5 ~ 6, and 7 ~ 8, the state class label can be determined.

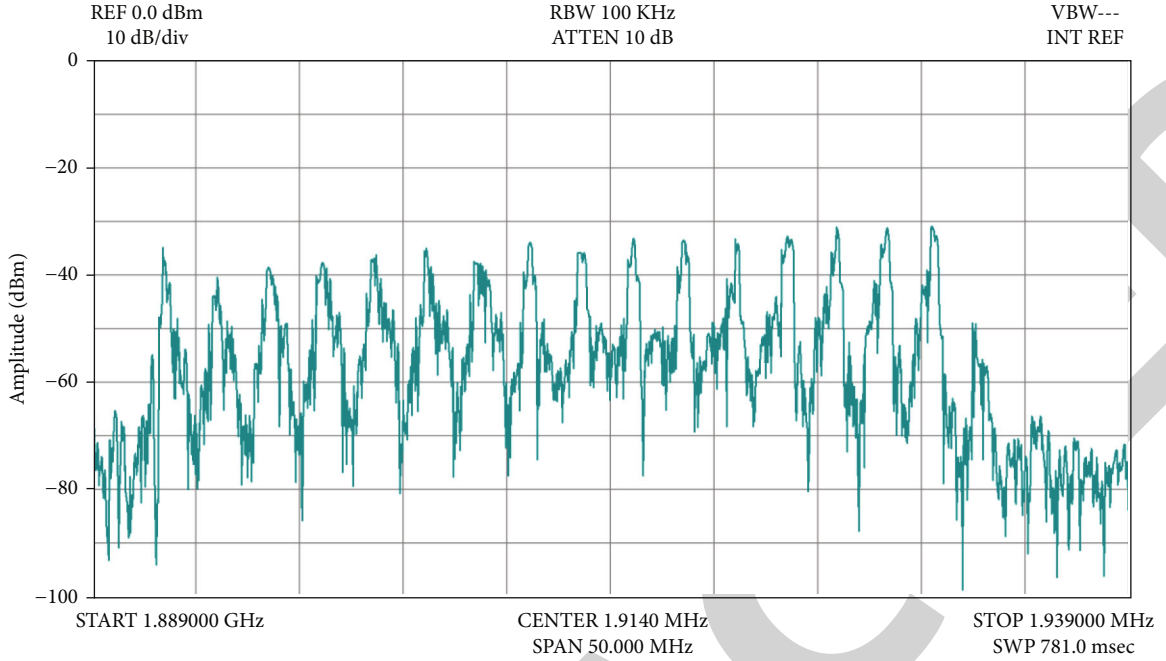


FIGURE 5: Spectrum of PHS mode.

It can be seen that the above-extracted feature data has obvious category features, which can correctly distinguish the four mode state features of signal source, but the resolution is not clear enough, and more detailed classifiers need to be built to distinguish.

**3.5. The Establishment of Classifier.** The traditional FCA is influenced by kernel function, and fuzzy selection is not of probability significance. At the same time, it is hard to classify nonlinear samples. Therefore, for known feature set  $\{x_i\}_{i=1}^n$ , category tag sequence is  $\{label_i\}_{i=1}^n$ ,  $i \in (1, 2, \dots, n)$ , and  $\omega_i$  is the weight parameter. The function of the soft interval classification optimization model of FCA is improved and constructed as follows:

$$\min_{\omega, b} \frac{1}{2} \|\omega\|^2 + K \sum_{i=1}^n \ell_{\log}(y_i(\omega^T x_i + b) - 1). \quad (5)$$

As shown in formula (5), where  $K > 0$  is a constant and  $\ell_{\log}(y_i(\omega^T x_i + b) - 1)$  is the logistic loss function, that is,  $\ell_{\log}(z) = \log(1 + \exp(-z))$ . The introduction of the pair rate regression model has the advantage of output prediction marker and probability parameter, which is suitable for multiclassification problems in application.

Therefore, it is equivalent to using the maximum likelihood method to solve the inner layer maximization in the Bayesian framework [19], as shown in

$$\max \ell(\omega, b) = \sum_{i=1}^n \log p(y_i | x_i; \omega, b). \quad (6)$$

Let  $\beta = (\omega, b)$ ,  $\hat{x} = (x; 1)$ , formula (7) can be trans-

formed into

$$\min \ell(\beta) = \sum_{i=1}^n \left( -y_i \beta^T \hat{x}_i + \log(1 + e^{\beta^T \hat{x}_i}) \right). \quad (7)$$

As shown in formula (7), it is a high-order continuous convex function of  $A$ . according to the Newton iterative method in convex optimization theory, the optimal solution  $\beta^* = \underset{\beta}{\operatorname{argmin}} \ell(\beta)$  can be obtained, and then, the weights  $\omega$  and  $b$  can be obtained. Furthermore, it is assumed that  $P(y_i | \omega)$  follows Bernoulli distribution and  $\omega$  follows Gauss prior distribution. In order to eliminate irrelevant noise component  $\sigma^2$ , the likelihood estimation probability model is obtained, as shown in

$$P(y_i | \omega) = \prod_{i=1}^n \sigma \{y(x_i; \omega)\}^{x_i} [1 - \sigma \{y(x_i; \omega)\}]^{1-x_i}. \quad (8)$$

In order to reduce the learning degree of the model, a penalty parameter  $\mathbb{R}(\omega_i | 0, \mu_i^{-1})$  is introduced for each weight to get the probability evaluation model.

$$P(\omega | \mu) = \prod_{i=0}^n \mathbb{R}(\omega_i | 0, \mu_i^{-1}). \quad (9)$$

As shown in formula (9),  $\mu = (\mu_0, \mu_1, \dots, \mu_n)^T$  is a sparse probability model constructed by  $n + 1$  dimensional hyper-parameters. It can be seen that the improved FCA based on pairwise regression fusion has the advantage of estimating the output prediction marker and adding probability parameters at the same time.

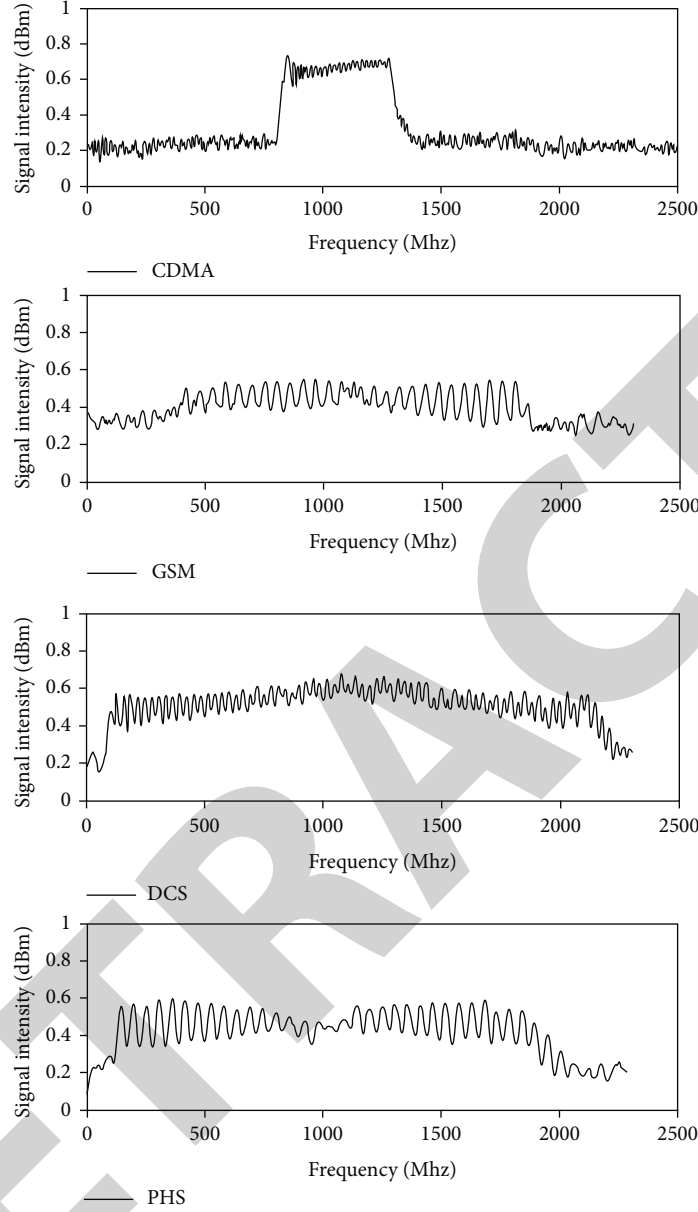


FIGURE 6: Spectrum normalization of four interference modes.

TABLE 1: Partial experimental characteristic data.

$RSSI_M$ (dBm)	$f_M$ ( $10^3$ MHz)	$f_{band}$ ( $10^3$ MHz)	$\psi$	$C$
-29.32	0.867	0.028	57.231	1
-30.51	0.873	0.027	56.538	1
-41.65	1.806	0.062	51.267	2
-40.37	1.847	0.058	50.324	2
-39.13	1.930	0.042	27.225	3
-38.42	1.923	0.045	26.881	3
-58.65	1.841	0.002	62.447	4
-60.31	1.831	0.001	63.617	4
...	...	...	...	...

3.6. *Optimization of Classification Processing.* Because the soft interval FCA classification model has high prediction cost, in order to reduce the overfitting risk of model training error, The SA algorithm is used to accelerate the convergence of FCA training process. The SA algorithm is easy to global optimization and to avoid local extremum, so it can achieve better global convergence.

Step 1. Initialization program, in which the initial temperature  $T_0$ , initial solution vector  $\psi_0$ , step size  $L_0 = 1$ , solution space vector dimension 3, the number of iterations 200, and termination threshold  $\xi = 1.0 \times 10^{-3}$ .

Step 2. The FCA model is used to calculate the initial solution  $\omega_i$ , and the SA algorithm is called with  $\omega_i$  as the initial point to generate a new point  $\omega'_i = \omega_i + \gamma L_0$  randomly, where  $\gamma \in (0, 1)$  is a random number and  $P(\omega_i | \mu)$  is calculated.

Step 3. The fitness  $\varphi_{(\omega,b)}$  is calculated by  $K$ -fold cross-validation, where the fold number  $K$  is set to 5, and the global optimal value is updated according to  $\varphi_{(\omega,b)}$ . If  $\varphi_{(\omega,b)} \leq 0$ , it has got the new solution is accepted. Otherwise, the new solution is accepted by probability  $p = \exp^{-\Delta\varphi_{(\omega,b)}^{(i)}/T}$ , where  $T$  is the current temperature control parameter. The annealing function is used to control the iteration speed  $T_n = \alpha T_{n-1}$ , and the annealing smoothing coefficient is set to  $\alpha = 0.8$ .

Step 4. When the iteration satisfies criterion  $T < \xi$  or the number of iterations reaches, the program exits, and the fine classification of samples is obtained.

**3.7. Train and Test.** In order to verify the resolution and generalization ability of the above models, the “reserve method” is also used to identify and verify the samples collected from different mode signal sources. Each mode state is sampled in 30 groups, and a total of 120 groups of experimental data are collected, and their characteristic parameters are extracted. In order to prevent data overtraining, 100 groups of each group of signal feature set are randomly selected for model training. Using 20 groups of feature samples as verification set for classifier test, the iteration number is 500, then stop threshold  $\varepsilon = 1.0 \times 10^{-5}$ , and model classification calculation to get confusion state matrix; according to the test results of confusion state matrix, the correct samples can be classified as table diagonal cumulative sum, a total of 18; the overall correct recognition rate can reach 90%, which can effectively identify the signals of four working modes.

Among them, the mode signal with identification error is DCS. The reason is that the spectrum characteristics of the signal source in this frequency band are close to that of the adjacent signal frequency band. When the signal strength of the detection signal source is close to that of the adjacent frequency band, there will be misjudgment, but the misjudgment rate is low. The confusion state matrix calculated from the model classification is shown in Table 2, which shows that the system can get enough accurate results for the specified signal source signal pattern identification.

## 4. Experimental Results and Analysis

**4.1. The Comparison of Identification Rate.** Through the SA44B spectrum receiver, the four modes of spectrum signals of the signal source carried by the indoor sports platform are collected indoors. Quantitative test experiments are carried out to verify the accuracy of feature selection of the SEEM algorithm and SA-FCA. The recognition rate is measured by extracting the percentage of correct samples in the unit number of features. The number of samples collected per unit is set to 200, and the proportion of correct eigenvalues and total eigenvalues is calculated, as shown in Figure 7. When the number of spectrum increases to 300, the highest recognition rate can reach 93.1%. Then, the feature selection ability of the SEEM algorithm decreases with the increase of the number of features. When the number of features increases to 400, extracted by SA-FCA, the maximum feature recognition rate reaches 96%. From the com-

TABLE 2: Disturbance source signal characteristic identification results.

Test status	The identification experiment results				
	CDMA	DCS	PHS	Mobile	Accuracy rate (%)
CDMA	5	0	0	0	100
DCS	0	4	0	1	90
PHS	0	0	5	0	100
Mobile	0	0	1	4	90

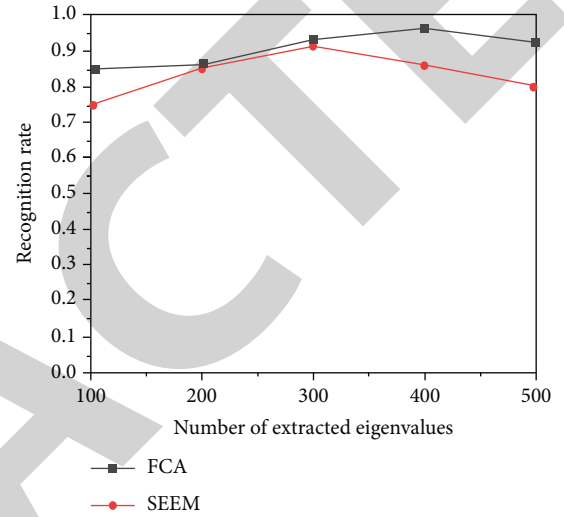


FIGURE 7: Comparison of SEEM and FCA identification rates.

parison chart of recognition rate, it can be seen that the larger the number of selected features is not the better, and the number of features shows a downward trend when the number of features reaches 400.

**4.2. Location Accuracy Analysis of Optimal Features.** Furthermore, the optimized spectrum eigenvalues of the signal source are used for positioning experiments to verify the influence of the optimization algorithm on the positioning accuracy. Traditional NN algorithm, KNN algorithm [20], SEEM algorithm, and improved FCA algorithm are compared in indoor positioning experiments, as shown in Figure 8. The improved FCA feature selection method can achieve 78% in the positioning error of 1.3m, which is 13% higher than the SEEM algorithm. The improved FCA feature selection method can achieve 83% in the positioning error of 1.5m, which is 8% higher than the SEEM algorithm.

## 5. Discussion

The classification analysis of eigenvalues extracted from radio wave signals is the basis of illegal signal identification. FCA model clustering is widely used as an unsupervised learning algorithm of the “hardening score” method. By adjusting the membership criterion, the individual feature vectors in the feature set are classified into subcategories of a cluster center one by one, and the similarity between

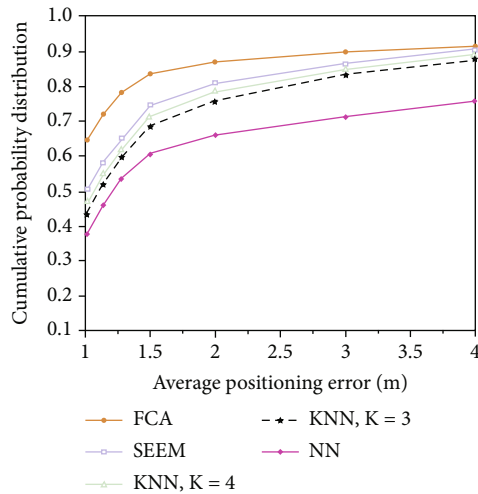


FIGURE 8: Cumulative error distribution of SEEM algorithm and FCA.

different categories is the smallest. According to this, through the fuzzy clustering identification of the characteristics of CDMA, GSM, DCS, and PHS four different mode signals, a small amount of sample data is used to test the effectiveness of extracting the categories of the eigenvalues of radio wave signals.

The FCA is a common classifier suitable for small sample sets and can also be extended to the field of multiclassification. Its core idea is to build a hyperplane model to classify the sample data in the feature space and remove the specific values. The difficulty is to separate the hyperplane close range samples with high confidence rate and maximum interval.

## 6. Conclusions and Future Work

Aiming at the problem of large positioning error caused by the working mode transformation of the signal source carried by the indoor sports platform, this paper first expounds the feature identification of the interference signal source from the new perspective of the spectrum detection and feature identification of the radio wave signal and studies the spectrum characteristics of the radio wave signal, after the denoising processing of the wavelet threshold method. Then, through the improved FCA model classification training and identification, the effect is better than the envelope method. Finally, the spectrum eigenvalues extracted from the identification are used for positioning. Indoor positioning experiments are carried out by traditional NN algorithm, KNN algorithm, seem algorithm, and improved FCA. The recognition rate of the collected samples is relatively ideal, and the positioning effect based on the feature data is better. In addition, there are other types of signal sources to be further studied, which require a large number of collected data to enrich the identification database, which need to be improved in the follow-up experiments.

## Data Availability

The data used to support the findings of this study are included in the article.

## Conflicts of Interest

The authors declare that they have no competing interests.

## Acknowledgments

This work was supported by the Key Research Projects Foundation of Xingtai City, China (No. 2020ZC012), and by the Youth Talent Projects Foundation of Xingtai City, China (No. 2021ZZ035).

## References

- [1] M. M. Harsha, R. H. Mulangi, and H. Kumar, "Analysis of bus travel time variability using automatic vehicle location data," *Transportation Research Procedia*, vol. 48, pp. 3283–3298, 2020.
- [2] S. Dewi and S. Sahriman, "Pemodelan statistical downscaling dengan regresi modifikasi jackknife ridge dummy Berbasis K-means untuk pendugaan curah hujan," *ESTIMASI Journal of Statistics and Its Application*, vol. 1, no. 12, pp. 19–28, 2021.
- [3] J. Park, H. Kim, J. Yoon, H. Kim, C. Park, and D. Hong, "Development of an ultrasound technology-based indoor-location monitoring service system for worker safety in ship-building and offshore industry," *Processes*, vol. 9, no. 2, p. 304, 2021.
- [4] S. Q. Zhang, Y. L. Dong, L. G. Zhang, B. Yan, and P. He, "Feature frequency extraction method based on mean envelope ITD and spectral kurtosis," *Jiliang Xuebao/Acta Metrologica Sinica*, vol. 38, no. 5, pp. 598–601, 2017.
- [5] K. Nonalinsavath, L. E. Nugroho, W. Widyawan, and K. Hamamoto, "Indoor location tracking system based on android application using bluetooth low energy beacons for ubiquitous computing environment," *Journal of Communications*, vol. 1, no. 1, pp. 572–576, 2020.
- [6] L. Dong, W. Wu, Q. Guo, M. N. Satpute, T. Znati, and D. Z. Du, "Reliability-aware offloading and allocation in multilevel edge computing system," *IEEE Transactions on Reliability*, vol. 70, no. 1, pp. 200–211, 2021.
- [7] Q. Yue and L. Zhang, "Two-sided matching for hesitant fuzzy numbers in smart intelligent technique transfer," *Mechanical Systems and Signal Processing*, vol. 139, article 106643, 2020.
- [8] M. K. Mishra, R. Renju, N. Mathew, C. Suresh Raju, M. R. Sujimol, and K. Shahana, "Characterization of GSAT-14 satellite Ka-band microwave signal attenuation due to precipitation over a tropical coastal station in the southern peninsular region of the indian subcontinent," *Radio Science*, vol. 55, no. 2, 2020.
- [9] S. Cao, X. Chen, X. Zhang, and X. Chen, "Combined weighted method for TDOA-based localization," *IEEE Transactions on Instrumentation and Measurement*, vol. 69, no. 5, pp. 1962–1971, 2020.
- [10] W. van Woensel, P. C. Roy, S. S. R. Abidi, and S. R. Abidi, "Indoor location identification of patients for directing virtual care: an AI approach using machine learning and knowledge-based methods," *Artificial Intelligence in Medicine*, vol. 108, article 101931, 2020.

- [11] Y. L. Chen, Y. C. Chang, and Y. L. Zeng, "An opportunistic large array concentric geographic routing algorithm with a relay node in wireless sensor networks," *Applied Mechanics & Materials*, vol. 764-765, pp. 838-842, 2015.
- [12] M. K. Khan, M. Shiraz, K. Zrar Ghafoor, S. Khan, A. Safaa Sadiq, and G. Ahmed, "EE-MRP: energy-efficient multistage routing protocol for wireless sensor networks," *Wireless Communications & Mobile Computing*, vol. 2018, article 6839671, pp. 1-13, 2018.
- [13] J. H. Choi, E. B. Cho, Z. Ghassemlooy, S. Kim, and C. G. Lee, "Visible light communications employing PPM and PWM formats for simultaneous data transmission and dimming," *Optical & Quantum Electronics*, vol. 47, no. 3, pp. 561-574, 2015.
- [14] H. el-Sayed, S. Sankar, M. Prasad et al., "Edge of things: the big picture on the integration of edge, IoT and the cloud in a distributed computing environment," *IEEE Access*, vol. 6, pp. 1706-1717, 2018.
- [15] E. Berriochoa, A. Cachafeiro, and J. M. García Amor, "Gibbs-Wilbraham oscillation related to an Hermite interpolation problem on the unit circle," *Journal of computational and applied mathematics*, vol. 344, pp. 657-675, 2018.
- [16] Y. Gao and Y. Chen, "Spectrum sensing exploiting the maximum value of power spectrum density in wireless sensor network," *Wireless Networks*, vol. 25, no. 4, pp. 1949-1964, 2019.
- [17] N. Shahid, I. H. Naqvi, and S. B. Qaisar, "Characteristics and classification of outlier detection techniques for wireless sensor networks in harsh environments: a survey," *Artificial Intelligence Review*, vol. 43, no. 2, pp. 193-228, 2015.
- [18] H. A. Chowdhury and M. S. Rahman, "Formant estimation from speech signal using the magnitude spectrum modified with group delay spectrum," *Acoustical Science and Technology*, vol. 42, no. 2, pp. 93-102, 2021.
- [19] H. Hunt, "Lightning location system detections as evidence: a unique bayesian framework," *IEEE Transactions on Geoscience and Remote Sensing*, vol. 59, no. 3, pp. 1848-1858, 2021.
- [20] J. Zhang, H. You, and R. Jia, "Reliability hazard characterization of wafer-level spatial metrology parameters based on LOF-KNN method," *Microelectronics Reliability*, vol. 107, article 113599, 2020.